






Article

# Calculating a Drop in Carbon Emissions in the Strait of Gibraltar (Spain) from Domestic Shipping Traffic Caused by the COVID-19 Crisis

Vanessa Durán-Grados <sup>1</sup>, Yolanda Amado-Sánchez <sup>1</sup> , Fátima Calderay-Cayetano <sup>1</sup>,  
Rubén Rodríguez-Moreno <sup>1</sup> , Emilio Pájaro-Velázquez <sup>1</sup> , Antonio Ramírez-Sánchez <sup>1</sup> ,  
Sofia I. V. Sousa <sup>2</sup> , Rafael A. O. Nunes <sup>2</sup>, Maria C. M. Alvim-Ferraz <sup>2</sup> and  
Juan Moreno-Gutiérrez <sup>1,3,\*</sup>

<sup>1</sup> Campus de Excelencia Internacional del Mar, College of Marine, Nautical and Radioelectronics Engineering, University of Cádiz, 11510 Puerto Real, Spain; vanesa.duran@uca.es (V.D.-G.); yolanda.amado@uca.es (Y.A.-S.); fatima.calderay@uca.es (F.C.-C.); ruben.rodriguezmoreno@uca.es (R.R.-M.); emilio.pajaro@uca.es (E.P.-V.); antonioramirez.sanchez@uca.es (A.R.-S.)

<sup>2</sup> LEPABE—Laboratory for Process Engineering, Environment, Biotechnology and Energy, Faculty of Engineering, University of Porto, Rua Dr. Roberto Frias, 4200-465 Porto, Portugal; sofia.sousa@fe.up.pt (S.I.V.S.); raonunes@fe.up.pt (R.A.O.N.); aferraz@fe.up.pt (M.C.M.A.-F.)

<sup>3</sup> School of Marine, Nautical and Radioelectronics Engineering, University of Cádiz, Polígono Río San Pedro, 11510 Puerto Real, Spain

\* Correspondence: juan.moreno@uca.es

Received: 16 October 2020; Accepted: 9 December 2020; Published: 11 December 2020



**Abstract:** As a consequence of the COVID-19 pandemic, the Spanish government declared a State of Emergency, and domestic passenger ship traffic was restricted in Spanish ports. This manuscript presents scenarios of emissions from domestic shipping traffic in the seas of the Strait of Gibraltar (Spain) over three months of the COVID-19 pandemic. Emissions were estimated for only 90 days of the pandemic, and two scenarios were studied: emissions while vessels were berthed at the Algeciras Port and emissions as a consequence of the interruption of passenger ship transportation in the Strait of Gibraltar. To this end, the authors' own model was used, which has near zero uncertainties. This model was used for the first time in this study and takes into account both meteorological and sea condition parameters, as well as the efficiency of the propulsion system. The manuscript concentrates on the emissions of greenhouse gases (GHGs), nitrogen oxides (NO<sub>x</sub>), sulphur oxides (SO<sub>x</sub>), carbon dioxide (CO<sub>2</sub>), and particulate matter (PM) from six Ro-Pax ships that ceased to operate. The main finding is that as a consequence of the pandemic, reductions of up to 12% were found in the Strait of Gibraltar in all the pollutants and GHGs when taking into account all international traffic, while the decrease in emissions from domestic traffic only reached 51%.

**Keywords:** shipping emissions; greenhouse gases; Strait of Gibraltar; COVID-19; SENEM model

## 1. Introduction

Based on the Order TMA /419/2020 of 18 May [1], starting at 00:00 on 17 March 2020, passengers on board Ro-Pax passenger ships and ships providing the regular line service between the Spanish peninsula and Ceuta were forbidden from disembarking. For this reason, all the Ro-Pax ferries from Algeciras to Ceuta (Spain) and from Tarifa (Spain) to Tangier (Morocco) were stopped and berthed at the port of Algeciras.

The COVID-19 pandemic resulted in a decrease in maritime shipping activity due to the large drop in the demand for cargo and oil. Many vessels were dry-docked or sailed at reduced speeds to cut fuel consumption [2].

COVID-19 was first identified on 30 December 2019, and was declared a global pandemic by the World Health Organization (WHO) on 11 March 2020 [3]. It resulted in drastic changes in energy use, with expected impacts on the emissions of greenhouse gases (GHGs) and pollutants. The changes in emissions associated with the lockdown were entirely due to reductions in the energy demand [4].

In this sense, pollution from ships is a significant contributor to global air pollution, which affects not only the ports themselves, but also nearby coastlines, since it is also carried for long distances over land and sea. The direct emissions from ships (known as precursor pollutants) are mainly comprised of CO<sub>2</sub>, NO<sub>x</sub>, SO<sub>x</sub>, CO, and particulate matter (PM).

SO<sub>x</sub> and NO<sub>x</sub> emissions are known to exacerbate the secondary formation of fine particulate matter, PM<sub>2.5</sub> [5]. NO<sub>x</sub> emissions from diesel engines also contribute regionally to increasing ozone (O<sub>3</sub>) levels. All of these compounds represent a major threat to human health. They are known to be closely related to both mortality and morbidity in young children, and to the respiratory infections and asthma that affect them [6]. For these reasons, pollutant-specific, location-specific, and source-specific models of health impacts are important and must be considered in the design of policies for the control of emissions, as demonstrated by Stefani et al. [7].

Based on inputs of meteorological data and source information like emission rates and stack height, air quality models are designed to characterize primary pollutants that are emitted directly into the atmosphere from anthropogenic sources (ships in this case). The problem is that air quality models and ship emissions inventories present many uncertainties. The use of air quality models entails significant sources of errors from inaccurate measurements, as is the case of PM<sub>2.5</sub> in epidemiological studies [8]. Thus, exposure assessment depends strongly on the accuracy of the emissions inventory and on the outcomes of the air quality model where a chemical transport model is included [9].

Since there is not yet a clear agreement on the definition of the parameters to be used in the different models, a ship's emissions inventory is a highly debated issue. Ship Traffic, Energy and Environment Model STEEM [10] and Ship Traffic Emission Assessment Model STEAM [11] are the most widely used models. They use a ship's identity, position, speed, and draught at a given time-stamp. These data are employed, together with the ship's technical specifications, to calculate time histories (known as inventories) of estimated fuel consumption and emissions. All of these data can also be obtained on board the vessel; they are compiled and reported daily in what is known as the ship's noon report.

Models were used in this study because, in the case of maritime transport, there are no systems in place for monitoring and quantifying GHG and pollutant emissions in real time. However, in the case of domestic Ro-Pax traffic (vessels that are used for freight vehicle transport alongside passenger accommodation) around the Strait of Gibraltar (North of Morocco included), ships usually prepare their noon reports every day, and the data from these are used to calculate emissions from ships through the models mentioned above.

In inventories of this type, the most difficult factor for calculating emissions is determining the power delivered by the main engine in real time. In the models used to date, this variable is measured exclusively from the recorded speed of the ship. In this sense, the International Maritime Organization IMO [12] proposed a new model, but it has not specified the procedure for the calculation of speed loss coefficients.

In order to reduce the range of uncertainties, this study used the authors' own model named the Ship's Energy Efficiency Model (SENEM) [13]. This model defines the procedure for the calculation of speed loss coefficients.

Because the prime focus is to study the impacts of ship-based emissions on urban air quality and human health in heavy-traffic regions, the objective of the study is to estimate the emissions from

ships (CO<sub>2</sub>, NMVOC, CH<sub>2</sub>, N<sub>2</sub>O, NO<sub>x</sub>, SO<sub>x</sub>, CO, and PM) as accurately as possible over 90 days of the COVID-19 pandemic in waters around the Strait of Gibraltar.

The SENEM model will be presented in more detail in the next subsection.

Concentrations of emissions were found to be four- or five-fold higher on coastlines where ships regularly pass by [14]. On a global scale, between 2007 and 2012, shipping accounted for 15%, 13%, and 2% of the respective annual emissions of NO<sub>x</sub>, SO<sub>x</sub>, and CO<sub>2</sub> from anthropogenic sources [15]. In the case of the Strait of Gibraltar, 1028 ton/km<sup>2</sup>/year of CO<sub>2</sub>, 25.46 ton/km<sup>2</sup>/year of NO<sub>x</sub>, and 8.20 ton/km<sup>2</sup>/year of SO<sub>x</sub> were emitted in 2007 [16], while in 2017, the emissions reached 1330 ton/km<sup>2</sup>/year of CO<sub>2</sub>, 24 ton/km<sup>2</sup>/year of NO<sub>x</sub>, and 11.60 ton/km<sup>2</sup>/year of SO<sub>x</sub> [17].

The results from the inventories published to date seem to present a high range of uncertainty, mainly because, as the next subsection shows, the calculation of the main engine load factor (LF) value falls within this range of uncertainty. Moreover, in the case of the study of Ro-Pax vessels, the matter of speed is even more complex. For this reason, this paper simulates a detailed analysis of vessel speeds when approaching or exiting ports. Since it would be necessary to simulate data on a port-by-port basis to be able to apply robust assumptions [18], the movements of six Ro-Pax ships were simulated.

Furthermore, the energy consumption and emissions produced by each ship's operation phase were simulated as real cases by a practical algorithm from each ship. These algorithms were used in the estimation of the two most important parameters on voyages: fuel consumption and emissions.

A study was performed of the decrease in emissions resulting from the ships being stopped and the emissions in ports while at berth during the pandemic (90 days). While the calculations of the effects while ships are not sailing were simulated, the effects of ships at berth are real calculations.

This paper describes both the increase in emissions while vessels were berthed at Algeciras Port during the COVID-19 pandemic and the estimated reduction in emissions as a consequence of these six ships not sailing in waters around the Strait of Gibraltar between three Spanish ports (Algeciras, Ceuta, and Tarifa) and Tangier for 90 days.

## 2. Materials and Methods

Four models were used for the simulation, which was performed through a detailed analysis of on-board data for each situation and navigation mode. According to data from the Automatic Identification System (AIS) in 2017, 82,490 ships (47,365 International Navigation) cruised the Strait of Gibraltar (warships, fishing vessels, tugs, auxiliary boats, and dredgers were not included). The 35,125 domestic voyages were for transporting passengers, cars, trucks, goods, etc. between the Iberian Peninsula and the North of Africa; of these, 13,165 were fast ferries. In this study, 2700 were analyzed because there was less traffic during the months of the lockdown that were studied (second half of March, April, May, and first half of June).

Two primary emission sources are found on every ship: the main engine (ME), which is used for ship propulsion, and the auxiliary engine (AE), which is for generating electricity on board. When a ship is at berth, only the AE is running.

The emissions were evaluated using data (Table 1) from six fast ferries that did not sail in waters around the Strait of Gibraltar for 90 days due to the pandemic.

The emissions were calculated (Equation (2)) by multiplying the energy delivered in kWh by the emission factors (EF) in g/kWh for each pollutant in question: CO<sub>2</sub>, CO, NO<sub>x</sub>, SO<sub>x</sub>, CH<sub>4</sub>, N<sub>2</sub>O, NMVOC, and PM in this case.

While other models [11,19] for calculating a ship's emissions only take into account the speed of the ship, this study utilized the SENEM, a new model that takes into account the wind direction and speed, wave direction and height, current influence, and waterjet efficiency—parameters that other models do not consider.

**Table 1.** Characteristics of the ships studied and power delivered by auxiliary engines (AEs) for each mode.

Ship Type/Rounds	$P_{reference}$ ME (kW) <sup>1</sup>	Total AE (kW)				Speed (knots) <sup>3</sup>	Length (m)	Breadth (m)	Draug. (m) <sup>4</sup>
		Installed	Cruis. <sup>2</sup>	Manv. <sup>2</sup>	Hot. <sup>2</sup>				
A/270	28,800	4800	720	2160	1440	37	101	26.6	4.2
B/450	28,800	4800	720	2160	1440	42	92	26	4.26
C/540	14,800	3600	540	1620	1080	37	83	13	3.2
D/450	28,304	4600	690	2070	1380	35	86	26	3.8
E/540	17,600	4000	600	1800	1200	35	77.5	26	2.72
F/450	20,240	4200	630	1890	1260	35	96	14.6	2.19

<sup>1</sup> ME Power 100% MCR, <sup>2</sup> engine load factor applied by Starcrest Vessel Boarding Program, <sup>3</sup> Max. speed ( $V_{reference}$ ),

<sup>4</sup> Max. Draught ( $t_{ref}$ ).

## 2.1. Theory/Calculation

Equation (1) [20] shows the procedure for calculating emissions when the ship is sailing, where the AE is also included.

$$Emissions(g) = \left(\frac{D}{v}\right) [(ME) * EF_{ME} + (AE) * EF_{AE}] \quad (1)$$

where:

*Emissions* : Total emissions in grams for the pollutant of interest.

*D* (miles): Distance that the ship travels within the study area.

*v* (knots): Average speed of the ship.

Activity time (hours):  $\left(\frac{D}{v}\right)$ .

*ME* (kW): Maximum continuous rating (MCR) of the main engine.

$LF_{ME}$  (fraction) : Load factor of the main engine as a fraction of the MCR.

SFOC: Specific fuel oil consumption in g/kWh.

*AE* (kW): Maximum continuous rating (MCR) of the auxiliary engine.

$LF_{AE}$  (%): Load factor of the auxiliary engine as a fraction of the MCR.

$EF_{ME}$  (g/kWh): Emission factor for the main engine for the pollutant of interest (this varies by engine type and fuel consumed rather than by activity mode).

$EF_{AE}$  (g/kWh): Emission factor for the auxiliary engine for the pollutant of interest.

As the MCR is known for each engine [21], the most important factor is the calculation of the load factor (LF). This is calculated according to Equation (2), and is necessary for calculating the main engine power delivered in real time (transient power).

$$LF = \frac{P_{transient}}{P_{reference}} \quad (2)$$

where:  $P_{reference}$  and  $P_{transient}$  are the power at 100% MCR and the instantaneous power for calculation, respectively.

### 2.1.1. ME Transient Power

For calculating the ME transient power, two options can be applied:

The first is by applying the current STEEM and STEAM models [11,19], where the LF is defined as being dependent only on the speed of the ships.

STEEM [19] uses Equations (2) and (3):

$$P_{transient} = P_{reference} \left(\frac{V_{transient}}{V_{reference}}\right)^3 \quad (3)$$

STEAM [11] uses Equation (4):

$$P_{transient} = \varepsilon_p * P_{installed} \left( \frac{V_{transient}}{V_{reference} + V_{safety}} \right)^3 \quad (4)$$

The IMO [12] uses Equation (5):

$$P_{transient} = \frac{P_{ref} \left( \frac{t_{transient}}{t_{ref}} \right)^{\left(\frac{2}{3}\right)} \left( \frac{V_{transient}}{V_{ref}} \right)^3}{\eta_w \eta_f} \quad (5)$$

where:  $P_{transient}$ ,  $V_{transient}$ , and  $t_{transient}$  are, respectively, the instantaneous power, speed, and draught at time  $t$  (all taken from Lloyd's Register of Ships, IHSF);  $P_{ref}$  is the reference power at speed  $V_{ref}$  and draught  $t_{ref}$ ;  $\eta_w$  is the modification of the propulsion efficiency due to weather; and  $\eta_f$  is the modification of the propulsion efficiency due to fouling.

This uses the Admiralty formula, which assumes that power is related to displacement to the power of  $2/3$ .

If the ship is new, then  $\eta_f = 1$ . If the ship is steaming at the reference draught ( $t_{ref}$ ), then  $t_{transient} = t_{ref}$ . For ideal sea and wind conditions, then  $\eta_w = 1$ . In these cases only, Equation (5) = Equation (3).

The second option involves applying the SENEM model [13], as defined by Equation (6), where the propulsion system efficiency,  $\eta_j$ , was considered as a variable value, and wind direction, wind speed, wave direction, and wave height were included. However, the influence of current was obviated by conducting round voyages and averaging the results for opposite directions.

This model takes into account and quantifies all the variables related to air and sea meteorological conditions, the state of maintenance of the hull and propeller, and the performance of the propulsion system. All of these variables have a direct influence on the power delivered by the main engines.

Because this new model significantly reduces the uncertainties that currently limit confidence in the emissions inventories of ships, its application is a novelty of this study (Equation (6)).

$$P_{transient} = \frac{P_{ref} \left( \frac{t_{transient}}{t_{ref}} \right)^{\left(\frac{2}{3}\right)} \left[ \left( \frac{V_{transient} + \Delta V_{wind \text{ and } waves} + \Delta V_{fouling} \pm \Delta V_{current}}{V_{ref}} \right)^n \right]}{\eta_j} \quad (6)$$

where:

$\Delta V_{wind \text{ and } waves}$  = Speed loss due to wind and waves;

$\Delta V_{fouling}$  = Speed loss due to fouling;

$\Delta V_{current}$  = Difference between speed on the surface and speed over the sea bottom;

$\eta_j$  = Efficiency of the propulsion system.

The study was performed in two directions, both taking and not taking into account the meteorological conditions and influence of the propulsion system.

The SENEM model [13] uses the Kwon method to predict speed loss due to added resistance in abnormal weather conditions (irregular waves and wind). This model was applied to the same ships analyzed in this study in 2017, and a value of  $\eta_w = 0.95$  was used for the worst weather conditions; this is the same value used to simulate bad weather conditions in this study.

For medium-sized, medium-speed ships such as the Ro-Pax ships in this study, we used  $n = 3.5$  [22].

The value of  $\eta_j$  (propulsion system efficiency) can be calculated using 1 as a basic value, which corresponds with the maximum efficiency value—usually 60%. From the curve obtained from the supplier, the value of  $\eta_j$  depends on the speed of the ship.

Thus,  $\eta_j$  is the efficiency of the propulsion system (equation of the type  $y = a + bx^2$ , where  $y$  is the efficiency of the propulsion system and  $x$  is the speed of the ship).

Because the same ships were studied as in the SENEM model used for validating the model, and a value of  $\eta_j = 0.85$  was used for the worst conditions (mode of maneuvering near port), the same value was used for this study.

In this method, the power will depend on  $\eta_j$  and  $\frac{V_{transient}}{V_{ref}}$ , and therefore,  $P_{transient}$  will have a double dependence on the speed of the ship.

For this study, only the  $\left(\frac{t_{transient}}{t_{ref}}\right)^{\left(\frac{2}{3}\right)}$  parameter was taken as a constant value.

The weather impact parameter aims to quantify the additional power requirements of the engine in realistic operating conditions. Based on other publications [23], a value of  $\eta_w = 0.95$  was used to simulate bad weather conditions.

The frictional resistance of the hull depends on the wetted area of the hull and on the specific frictional resistance coefficient. Friction increases with fouling of the hull surface, e.g., due to the growth of algae, sea grass, barnacles, and other matter. An average increase in total resistance of 9% (constant over time) was applied for all ships [12]. Another study [24] showed that a daily consumption increase of 10% was induced. In Equation (6), a value of  $\eta_f = 0.98$  was used.

Because all of the ships analyzed are propelled by a waterjet system, the effect of the propeller's fouling condition, defined in Equation (5), was not taken into account.

Finally, when all the efficiency parameters are defined, Equation (6) shows the global efficiency ( $\eta_g$ ) for the worst weather, hull, and performance propulsion system conditions:

$$\eta_g = 0.85 \times 0.95 \times 0.98 = 0.79$$

The fuel consumption and emissions were calculated as a product of the number of round trips (2700 in this case), sailing time per round trip, engine size, engine load factor, and energy consumption/emission factor.

### 2.1.2. AE Power

The auxiliary power demands vary depending on the mode of operation (i.e., cruising, maneuvering, at berth).

Two ways were used to calculate the energy consumption and emissions for auxiliary engines.

#### Ships at Sea

When the ships are at sea, the power delivered by the AE depends on the type of ship and the navigation mode. For the case of fast ferries, Table 1 shows the delivered power values for each mode; the LF applied was obtained from the Starcrest Vessel Boarding Program [25].

#### Ships at Berth

In the case of ships moored at berth, the AE provides the energy they need for moving ramps inside the hold, the refrigeration of containers of goods, air conditioning of the passages, and interior lighting. In this case, energy was only required for interior lighting, and Equation (7) was used.

$$DE = BT \times (P_{delivered,r}) \times EF \quad (7)$$

where:

DE: Daily emissions (g);

BT: Berthing time (24 h);

$P_{delivered}$ : Average power delivered by the AE for each ship (kW);

EF: Emission factor for the pollutant studied (g/kWh).

The emissions during the lockdown were calculated as the total emissions from six ships at berth per day multiplied by ninety days using the bottom-up method according to Equation (5), taking into

account that the six ships were berthed for 24 h every day for 90 days.  $P_{\text{delivered}}$  is described in Table 2 as Power(kW).

**Table 2.** Total emissions by day and during the COVID-19 lockdown (90 days) of each pollutant from the auxiliary engines (kg) of ships at berth in Algeciras Port.

Ship Type	Power (kW)	CO <sub>2</sub>	CH <sub>4</sub>	N <sub>2</sub> O	NMVOG	CO	SO <sub>x</sub>	NO <sub>x</sub>	PM
A	190 <sup>1</sup>	2959	0.036	0.132	0.042	0.061	10.48	47.65	1.6
	1440 <sup>2</sup>	22,429	0.272	1	0.318	0.46	79.43	342.13	11.48
B	40 <sup>1</sup>	623	0.0075	0.027	0.009	0.0129	2.2	10	0.33
	1440 <sup>2</sup>	22,428	0.27	0.972	0.324	0.46	79.2	360	11.88
C	42 <sup>1</sup>	654	0.008	0.029	0.0099	0.013	2.3	10.5	0.35
	1080 <sup>2</sup>	16,808	0.2	0.745	0.254	0.33	59.11	269.8	9
D	45 <sup>1</sup>	701	0.0085	0.031	0.01	0.014	2.48	11.28	0.37
	1380 <sup>2</sup>	21,493	0.26	0.95	0.30	0.429	76	346	11.34
E	42 <sup>1</sup>	654	0.008	0.029	0.0099	0.013	2.3	10.5	0.35
	1200 <sup>2</sup>	18,704	0.228	0.83	0.283	0.37	65.8	300	10
F	40 <sup>1</sup>	623	0.0075	0.027	0.009	0.0129	2.2	10	0.33
	1260 <sup>2</sup>	19,624	0.236	0.85	0.283	0.4	69.3	315	10.4
<b>TOTAL Daily<sup>1</sup></b>		6214	0.0755	0.275	1.84	2.52	21.96	99.93	3.33
<b>TOTAL Daily<sup>2</sup></b>		121,486	1.466	5.34	15	20.6	428.8	1932.9	64.1
<b>TOTAL<sup>1</sup></b>		559,260	6.80	24.75	166.30	227.32	1976.4	8993.70	299.7
<b>TOTAL<sup>2</sup></b>		10,933,740	131.9	480.6	1350	1854	38,592	173,961	5769

<sup>1</sup> During the COVID-19 lockdown. <sup>2</sup> Normal conditions.

For the second case—ships operating in waters around the Strait of Gibraltar—the SENEM model was applied through simulation.

## 2.2. Emission Factors

Finally, the total emissions (in g) of each pollutant of interest were obtained by multiplying the energy consumption (kWh) by the EF. Table 3 shows the values for all types of fuel used in these kinds of ships [26].

It is very important to take into account that while mass emissions tend to decrease as vessel speeds and engine loads decrease, emission factors increase. Thus, the EF is not a constant value because it depends on the main engine load factor; for ME load factors of less than 20%, Equation (8) (Table 4) was applied [10]:

$$y = a \times \text{LF}^{-x} + b \quad (8)$$

where:

y = emissions in g/kWh;

a = coefficient;

b = intercept;

x = exponent (negative).

**Table 3.** Typical emission factors for a range of engines and fuel types (g/kWh) (Goldsworthy and Galbally, 2011). While ships were at berth during the pandemic, only marine diesel oil (MDO) was used.

Engine Type	Fuel Type	EMISSION FACTORS (g/kWh)					
		CO <sub>2</sub>	CO	SO <sub>x</sub>	NO <sub>x</sub>	PM <sub>10</sub>	PM <sub>2.5</sub>
MSD Main	HFO	659.3	1.1	11.5	14	1.5	1.46
MSD AUX	HFO	702.6	1.1	12.3	14.7	1.5	1.46
MSD AUX	MDO	661.4	1.1	2.2	13.9	0.38	0.35

**Table 4.** Factors from Equation (6).

Pollutant	Exponent	Intercept (b)	Coefficient (a)
PM	1.5	0.25	0.0059
NO <sub>x</sub>	1.5	10.45	0.1255
CO	1.0	0.15	0.8378
HC	1.5	0.39	0.0667

### 3. Results

The results were analyzed in two ways: ships at berth in the port of Algeciras and ships sailing through the Strait of Gibraltar in a “no pandemic” case.

In the first case, Table 2 shows the total daily emissions over the 90 days of the COVID-19 pandemic for all the pollutants studied, both while the ships were at berth in the port of Algeciras and under normal conditions (no pandemic) by using the data of the power delivered based on LF values from the Starcrest Vessel Boarding Program. The results for all the pollutants analyzed are based on the emission factor values from Table 5 [27].

**Table 5.** Emission factors in units of g/kWh (marine diesel oil used).

CO <sub>2</sub>	CH <sub>4</sub>	N <sub>2</sub> O	NMVOC	CO	SO <sub>x</sub>	NO <sub>x</sub>	PM
649	0.008	0.029	0.4	0.54	2.3	10.5	0.35

Figure 1 shows the actual power and energy delivered by the ME, which were obtained per round trip in cruising mode, the mode of maneuvering near port, and the mode of maneuvering into the port, respectively. Equation (5) was used.

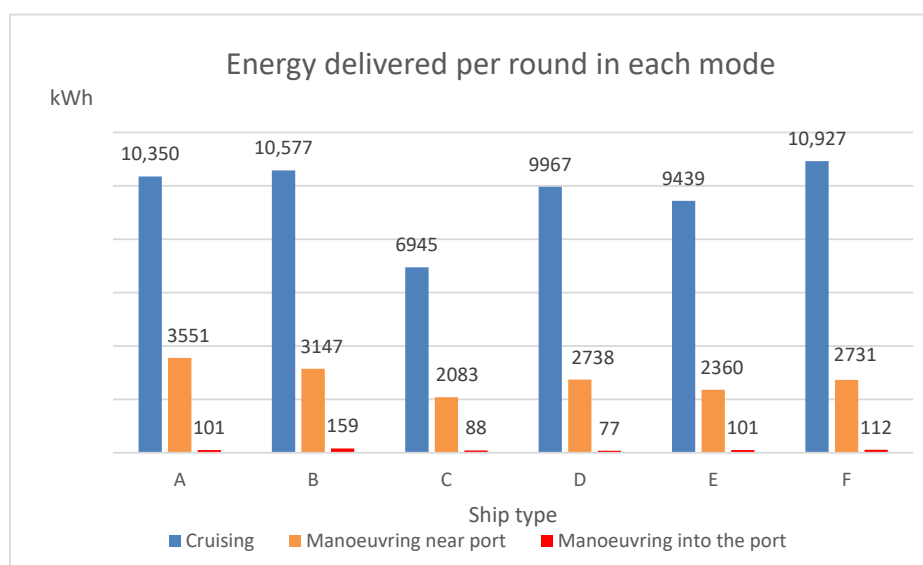


**Figure 1.** Energy delivered from the main engine (ME) (kWh) per round trip, and mode.



Figure 2 shows the energy consumed by the AE for all modes per round trip, taking into account the average for each navigation mode, with data from on board and Table 1.

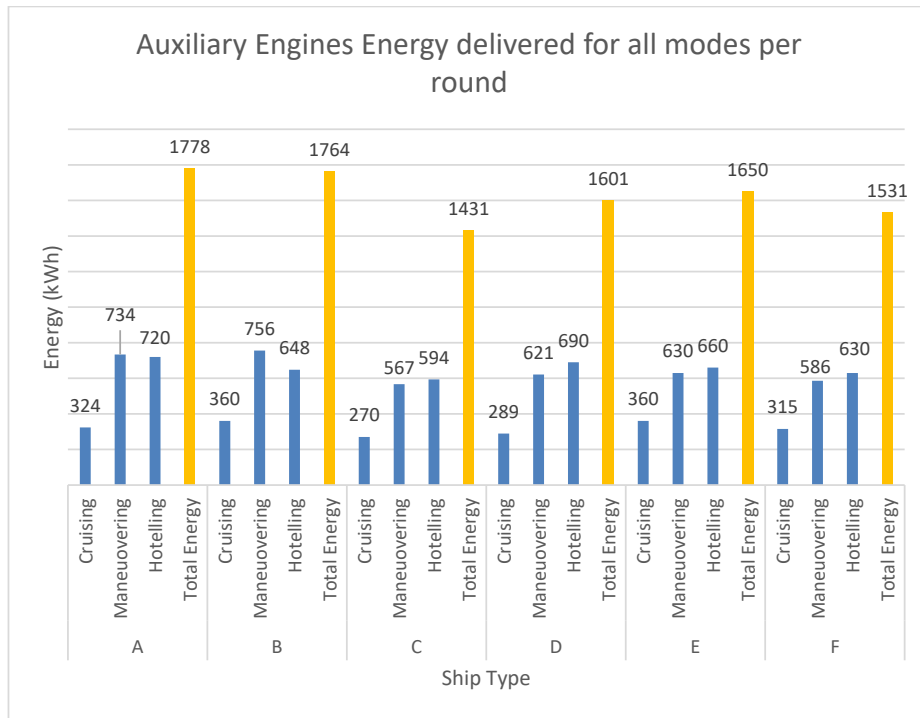


Figure 2. Energy delivered from the AE (kWh) per ship, round trip, and mode.

Figure 3 shows the total energy consumption per round trip for both the ME and AE.

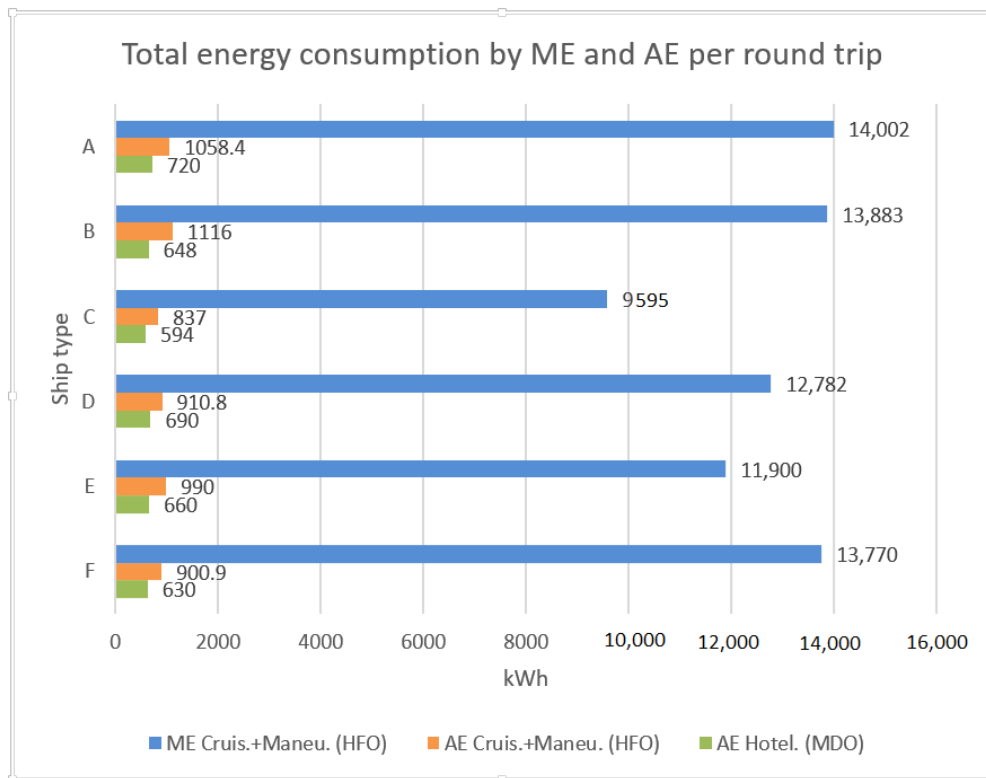
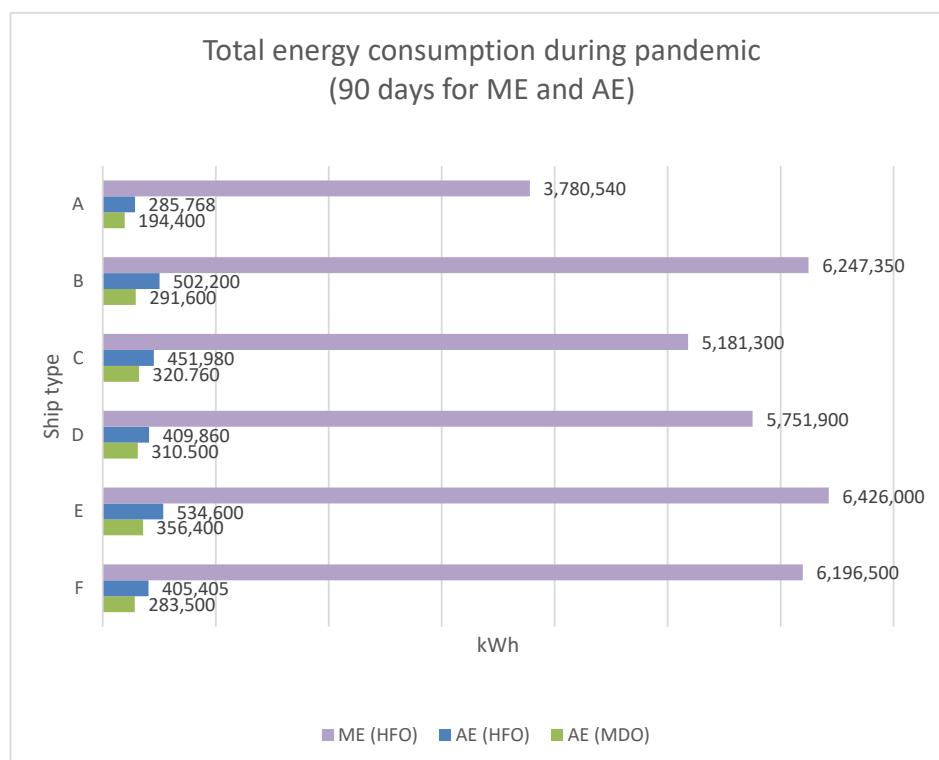


Figure 3. Total energy per round trip in calm conditions for the ME and AE (kWh).

Figure 4 shows the total energy consumption per round trip during the pandemic for heavy fuel oil (HFO) and marine diesel oil (MDO), calculated using Equation (5).



**Figure 4.** Total energy consumption during the pandemic (90 days) by ME and AE.

Figure 5 shows the total energy consumption during the same time for the ME and AE (kWh), taking into account the worst weather, hull, and performance propulsion system conditions. In this case, Equations (5) and (6) were used.

Table 6 shows the decrease in total emissions due to domestic shipping traffic not sailing around the waters of the Strait of Gibraltar during the 90 days of the pandemic under normal conditions.

**Table 6.** Decrease in total emissions (tons) due to domestic shipping traffic not sailing around the waters of the Strait of Gibraltar during the pandemic (90 days).

TYPE	Fuel Type	CO <sub>2</sub>	CO	SO <sub>x</sub>	NO <sub>x</sub>	PM <sub>10</sub>	PM <sub>2.5</sub>
A	ME (HFO)	2492.5	4.2	43.5	52.9	5.7	5.5
	AE (HFO)	200.78	0.3	3.5	4.2	0.4	0.4
	AE (MDO)	128.9	0.2	0.4	2.7	0.1	0.1
B	ME (HFO)	4118.9	6.9	71.8	87.5	9.4	9.1
	AE (HFO)	352.8	0.6	6.2	7.4	0.8	0.7
	AE (MDO)	192.9	0.3	0.6	4.1	0.1	0.1
C	ME (HFO)	3416	5.7	59.6	72.5	7.8	7.6
	AE (HFO)	317.6	0.5	5.6	6.6	0.7	0.7
	AE (MDO)	212.2	0.4	0.7	4.5	0.1	0.1
D	ME (HFO)	3792.2	6.3	66.1	80.5	8.6	8.4
	AE (HFO)	288	0.5	5	6	0.6	0.6
	AE (MDO)	205.4	0.3	0.7	4.3	0.1	0.1

Table 6. Cont.

TYPE	Fuel Type	CO <sub>2</sub>	CO	SO <sub>x</sub>	NO <sub>x</sub>	PM <sub>10</sub>	PM <sub>2.5</sub>
E	ME (HFO)	4236.7	7.1	73.9	90	9.6	9.4
	AE (HFO)	375.6	0.6	6.6	7.9	0.8	0.8
	AE (MDO)	235.7	0.4	0.8	5	0.1	0.1
F	ME (HFO)	4085.4	6.8	71.3	86.8	9.3	9
	AE (HFO)	284.8	0.4	5	6	0.6	0.6
	AE (MDO)	187.5	0.4	0.6	3.9	0.1	0.1
TOTAL ME		18,349.5	37	386.2	470.2	50.4	49
TOTAL AE		6773.9	4.9	35.7	62.5	4.5	4.4
TOTAL		25,123.4	41.9	421.9	532.7	54.9	53.4

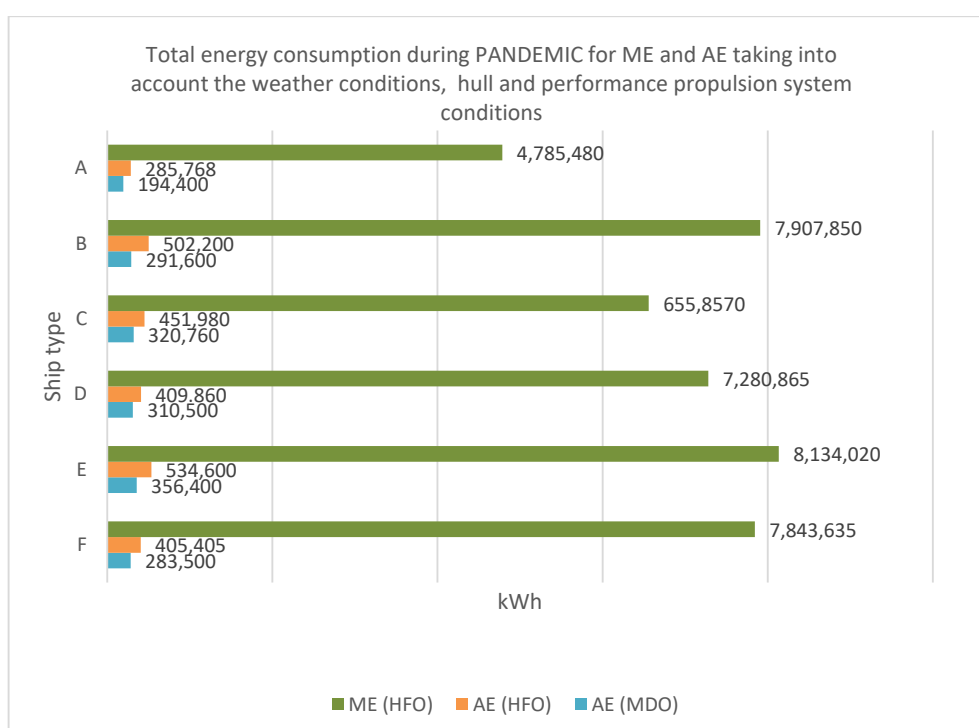


**Figure 5.** Total energy consumption during the pandemic for ME and AE taking into account the weather, hull, and performance propulsion system conditions”.

Meanwhile, Table 7 shows the decrease in total emissions (tons) due to domestic shipping traffic not sailing around the waters of the Strait of Gibraltar during the 90 days of the pandemic, taking into account the worst weather, hull, and performance propulsion system conditions.

**Table 7.** Decrease in total emissions (tons) due to domestic shipping traffic not sailing around waters of the Strait of Gibraltar during the pandemic (90 days), taking into account the worst weather, hull, and performance propulsion system conditions.

TYPE	CO <sub>2</sub>	CO	SO <sub>x</sub>	NO <sub>x</sub>	PM <sub>10</sub>	PM <sub>2.5</sub>
TOTAL ME	23,227.2	46.83	488.86	595.1	63.79	62
TOTAL AE	6773.9	4.9	35.7	62.5	4.5	4.4
TOTAL	30,001	51.73	524.56	657.6	68.29	66.4

Finally, Tables 8 and 9 compare the results of this study with others from the literature [16,17] for domestic passenger traffic only.

**Table 8.** Decreases in total emissions found in two published studies [16,17] and this paper (tons).

Publications	CO <sub>2</sub>	CO	SO <sub>x</sub>	NO <sub>x</sub>	PM <sub>10</sub>
Moreno 90 days	237,786	325.25	2456.5	6231.5	2010.25
Nunes 90 days	285,950	81.31	614.12	1557.87	502.56
COVID-19	30,001	51.73	524.56	657.6	68.22

**Table 9.** Results from two published studies [16,17] and this paper in the case of one year of the pandemic.

Publications	CO <sub>2</sub>	CO	SO <sub>x</sub>	NO <sub>x</sub>	PM <sub>10</sub>
Moreno (2015)	951,145	1301	9826	24,926	8041
Nunes (2017)	1,143,800	1969.4	9976	20,640	2597.2
COVID-19 (Simulated 2020)	120,004	206.92	2098.24	2630.4	273.16

#### 4. Discussion

This article presents the results of the study that the authors performed in the port of Algeciras and the Strait of Gibraltar (Spain), which covered six Ro-Pax ferries propelled by waterjet systems operating over the course of 90 days. The total emissions from the Ro-Pax ships over 90 days of the COVID-19 pandemic were compared with those emitted under normal conditions.

The emission values from ships at sea decreased substantially during the COVID-19 pandemic. We calculated decreases of 10% for CO<sub>2</sub> compared with Nunes' study [17] and 12% compared with Moreno's study [16], both of which were conducted before the COVID-19 pandemic. For the remaining pollutants, the differences show similar values.

In the case of ships at berth, the differences are greater, with emissions up to 95% lower. This is because when ships are at berth, there is no energy consumption due to the movement of ramps, refrigeration of containers of goods, air conditioning of the passages, etc.; only interior lighting is used.

In the case of ships in all navigation modes, when the propulsion system efficiency, wind direction, wind speed, wave direction, and wave height were considered as variable values, the values found were up to 17% higher for most of the pollutants emitted compared with those under calm conditions. The authors' own model was applied for the first time in this study.

Taking into account all the international traffic around the Strait of Gibraltar, the results show a 12% drop in the pollutants emitted by ships as a result of six ships being docked. Meanwhile, considering all domestic traffic and not only passenger traffic, the decrease in emissions found was 51%.

A study from the European Maritime Safety Agency (EMSA) [28] showed a traffic density map for all the ships, tankers, cargo vessels, and passenger ships in European waters in October 2019 and October 2020. The main conclusion was that traffic in and around EU waters was not heavily affected, apart from the decrease in the number of passenger ships.

#### 5. Conclusions

This study showed that in the port of Algeciras, there was no increase in emissions even though ships were continuously docked during the lockdown (90 days). This is because the energy required by their auxiliary engines is very low when the ships are at berth in comparison with when they are in an operating mode.

For the ships sailing in waters around the Strait of Gibraltar, the results obtained suggest that domestic traffic through the Strait of Gibraltar has great importance for both energy consumption by and emissions from maritime transport. As a result of only six Ro-Pax vessels being inactive,

the emissions of some pollutants decreased by up to 12% when taking into consideration all the traffic around the Strait of Gibraltar.

**Author Contributions:** Methodology, V.D.-G.; writing—review and editing, J.M.-G; resources, Y.A.-S. and F.C.-C.; original draft preparation R.R.-M., E.P.-V. and A.R.-S.; formal analysis S.I.V.S., R.A.O.N. and M.C.M.A.-F. All authors have read and agreed to the published version of the manuscript.

**Funding:** This research was funded by Consejería de Salud, Junta de Andalucía, Spain: 0094 2017.

**Acknowledgments:** This work was financially supported by: project UIDB/00511/2020 of the Laboratory for Process Engineering, Environment, Biotechnology and Energy—LEPABE—funded by national funds through the FCT/MCTES (PIDDAC) and project EMISSHIP PTDC/CTA-AMB/32201/2017, funded by FEDER funds through COMPETE2020—Programa Operacional Competitividade e Internacionalização (POCI) and by national funds (PIDDAC) through FCT/MCTES. Rafael A.O. Nunes thanks the individual research grant SFRH/BD/146159/2019, funded by the Portuguese Foundation for Science and Technology (FCT). Sofia I.V. Sousa thanks the Portuguese Foundation for Science and Technology (FCT) for the financial support of her work contract through the Scientific Employment Stimulus—Individual Call—CEECIND/02477/2017.

**Conflicts of Interest:** The authors declare no conflict of interest.

## References

1. BOE núm. 141, de 19 de mayo de 2020, Páginas 33496 a 33503. *Ministerio de Transportes, Movilidad y Agenda Urbana*. BOE-A-2020-5125. Available online: <https://www.boe.es/eli/es/o/2020/05/18/tma419> (accessed on 30 April 2020).
2. Teter, J.; The Covid-19 Crisis and Clean Energy Progress. Tracking Transport. *Tracking Clean Energy Progress*. 2020. Available online: <https://www.iea.org/reports/the-covid-19-crisis-and-clean-energy-progress> (accessed on 24 June 2020).
3. Cucinotta, D.; Vanelli, M. WHO Declares COVID-19 a Pandemic. *Acta Biomed.* **2020**, *91*, 157–160. [[CrossRef](#)] [[PubMed](#)]
4. Le Quéré, C.; Jackson, R.B.; Jones, M.W.; Smith, A.J.P.; Abernethy, S.; Andrew, R.M.; De-Gol, A.J.; Willis, D.R.; Shan, Y.; Canadell, J.G.; et al. Temporary reduction in daily global CO<sub>2</sub> emissions during the COVID-19 forced confinement. *Nat. Clim. Chang.* **2020**, *10*, 647–653. [[CrossRef](#)]
5. Deniz, C.; Durmuşoğlu, Y. Estimating shipping emissions in the region of the Sea of Marmara, Turkey. *Sci. Total. Environ.* **2008**, *390*, 255–261. [[CrossRef](#)]
6. World Health Organization. *Health Indicators of Sustainable Energy in the Context of the Rio+20 UN Conference on Sustainable Development. Initial Findings from a WHO Expert Consultation*; World Health Organization: Geneva, Switzerland, 2012.
7. Penn, S.L.; Arunachalam, S.; Woody, M.C.; Heiger-Bernays, W.; Tripodis, Y.; Levy, J.I. Estimating State-Specific Contributions to PM<sub>2.5</sub> - and O<sub>3</sub> -Related Health Burden from Residential Combustion and Electricity Generating Unit Emissions in the United States. *Environ. Health Perspect.* **2017**, *125*, 324–332. [[CrossRef](#)]
8. Matthias, V.; Bewersdorff, I.; Aulinger, A.; Quante, M. The contribution of ship emissions to air pollution in the North Sea regions. *Environ. Pollut.* **2010**, *158*, 2241–2250. [[CrossRef](#)] [[PubMed](#)]
9. Müller, D.; Uibel, S.; Takemura, M.; Groneberg, D.A.; Groneberg, D.A. Ships, ports and particulate air pollution - an analysis of recent studies. *J. Occup. Med. Toxicol.* **2011**, *6*, 31. [[CrossRef](#)]
10. EPA-420-R-10-013. Proposal to Designate an Emission Control Area. 2010. Available online: <http://www.epa.gov/otaq/regs/nonroad/marine/ci/420r10013.pdf> (accessed on 15 April 2020).
11. Jalkanen, J.P.; Brink, A.; Kalli, J.; Pettersson, H.; Kukkonen, J.; Stipa, T. Modelling System for the Exhaust Emissions of Marine Traffic and its Application in the Baltic Sea Area. *Atmos. Chem. Phys.* **2009**, *9*, 9209–9223. [[CrossRef](#)]
12. Smith, W.P.; Jalkanen, J.P.; Anderson, B.A.; Corbett, J.J.; Faber, J.; Hanayama, S.; O’Keeffe, E.; Parker, S.; Johansson, L.; Aldous, L.; et al. *Third IMO GHG Study*; International Maritime Organization (IMO): London, UK, June 2014.
13. Moreno-Gutiérrez, J.; Durán-Grados, V. Calculating ships’ real emissions of pollutants and greenhouse gases: Towards zero uncertainties. *Sci. Total Environ.* **2021**, *750*, 141471. [[CrossRef](#)] [[PubMed](#)]
14. Endresen, Ø.; Sørgård, E.; Behrens, H.L.; Brett, P.O.; Isaksen, I.S.A. A historical reconstruction of ships’ fuel consumption and emissions. *J. Geophys. Res. Space Phys.* **2007**, *112*, 301. [[CrossRef](#)]

15. European Climate Pact. Energetic Strategy 2030. Available online: <https://ec.europa.eu/clima/policies/eu-climate-action/pact.2020> (accessed on 25 May 2020).
16. Moreno-Gutiérrez, J.; Calderay, F.; Saborido, N.; Boile, M.; Valero, R.R.; Durán-Grados, V. Methodologies for estimating shipping emissions and energy consumption: A comparative analysis of current methods. *Energy* **2015**, *86*, 603–616. [[CrossRef](#)]
17. Nunes, R.A.O.; Alvim-Ferraz, M.C.M.; Martins, F.G.; Calderay-Cayetano, F.; Durán-Grados, V.; Moreno-Gutiérrez, J.; Jalkanen, J.-P.; Hannuniemi, H.; Sousa, S. Shipping emissions in the Iberian Peninsula and the impacts on air quality. *Atmos. Chem. Phys. Discuss.* **2020**, *20*, 9473–9489. [[CrossRef](#)]
18. Defra. *UK Ship Emissions Inventory*; Final Report November; Defra: Marsham Street, London, UK, 2010.
19. U.S. EPA. *Inventory of U.S. Greenhouse Gas Emissions and Sinks: 1990–2012*; U.S. EPA: Washington, DC, USA, 2014.
20. Trozzi, C.; Lauretis, R. *Air Pollutant Emission Inventory Guidebook*; European Environment Agency: Copenhagen, Denmark, 2013.
21. Eyring, V.; Köhler, H.W.; Van Aardenne, J.; Lauer, A. Emissions from international shipping: 1. The last 50 years. *J. Geophys. Res. Space Phys.* **2005**, *110*, 110. [[CrossRef](#)]
22. MAN Diesel & Turbo, Copenhagen, Denmark. Basic Principles of Ship Propulsion. December 2011. Available online: <https://spain.mandieselturbo.com/docs/librariesprovider10/sistemas-propulsivos-marinos/basic-principles-of-ship-propulsion.pdf?sfvrsn=2> (accessed on 1 April 2020).
23. Durán-Grados, V.; Mejías, J.; Musina, L.; Moreno-Gutiérrez, J. The influence of the waterjet propulsion system on the ships' energy consumption and emissions inventories. *Sci. Total Environ.* **2018**, 496–509. [[CrossRef](#)] [[PubMed](#)]
24. Luo, S.; Ma, N.; Hirakawa, Y. Evaluation of resistance increase and speed loss of a ship in wind and waves. *J. Ocean Eng. Sci.* **2016**, *1*, 212–218. [[CrossRef](#)]
25. Starcrest Consulting Group, LLC. *Port-Wide Baseline Air Emissions Inventory*; Starcrest Consulting Group, LLC: Port of Los Angeles, CA, USA, 2005.
26. Goldsworthy, L.C.; Renilson, M.R. Ship Engine Exhaust Emission Estimates for Port of Brisbane. *Air Qual. Clim. Chang.* **2013**, *47*, 26–36.
27. ENTEC 2002 and IVL 2004 Auxiliary Engine Emission Factors. IVL. Methodology for Calculating Emissions from Ships: Update on Emission Factors 2004. Available online: [https://www.researchgate.net/publication/237764562\\_Methodology\\_for\\_calculating\\_emissions\\_from\\_ships\\_1\\_Update\\_of\\_emission\\_factors](https://www.researchgate.net/publication/237764562_Methodology_for_calculating_emissions_from_ships_1_Update_of_emission_factors) (accessed on 10 December 2020).
28. EMSA. COVID-19—Impact on Shipping; European Maritime Safety Agency. Available online: <http://www.emsa.europa.eu> (accessed on 10 December 2020).

**Publisher's Note:** MDPI stays neutral with regard to jurisdictional claims in published maps and institutional affiliations.



© 2020 by the authors. Licensee MDPI, Basel, Switzerland. This article is an open access article distributed under the terms and conditions of the Creative Commons Attribution (CC BY) license (<http://creativecommons.org/licenses/by/4.0/>).